Microscopy and Microanalysis, **31** (7), 2025, 1994–1997
https://doi.org/10.1093/mam/ozaf048.998

Microscopy AND Microanalysis

Proceedings

Characterization of Diamond-like Carbon Coatings under Extreme Service Conditions

Cristina Jiménez-Marcos[1], Julia Claudia Mirza-Rosca[1,2,*], Dorin-Ioan Feldiorean[3], and Mircea Horia Ţierean[2]

[1]*Department of Mechanical Engineering, University of Las Palmas de Gran Canaria, Las Palmas de Gran Canaria, Spain.*
[2]*Materials Engineering and Welding Department, Transilvania University of Brasov, Brasov, Romania*
[3]*Dürkopp Adler SRL, Sangeorgiu de Mures, Romania*

*Corresponding author: julia.mirza@ulpgc.es

16MnCr5 steel is a popular material in industrial applications due to its mechanical strength, ductility, and heat treatment ability. Its composition of carbon, manganese, and chromium makes it suitable for wear-resistant components like gears, shafts, and camshafts. However, it has limitations under extreme conditions like repetitive movements or corrosive environments, reducing its performance and service life. To overcome these limitations, advanced coatings like diamond-like carbon (DLC) have been developed. DLC has a hybrid structure, featuring sp3 (diamond) and sp2 (graphite) carbon bonds, making it suitable for various industries [1].

DLC coatings form a low-friction [2], high wear-resistant layer on mechanically active surfaces [3], making them ideal for tribological applications [4]. In the biomedical field, DLC coatings are ideal for implants and surgical instruments due to their chemical inertness and biocompatibility [5]. In the electronics industry, DLC coatings protect sensitive devices against scratches and impacts [6].

Optimization of DLC coatings can be achieved through structural modifications and the use of dopants like nitrogen [7], silicon [8], chromium [9], or tungsten [10]. In summary, DLC materials offer an advanced solution to improve the performance of 16MnCr5 steel under extreme conditions. This study aims to determine the microstructure, corrosion resistance, and mechanical properties of three DLC samples with different heat treatment temperatures for use in different industrial fields under extreme conditions.

The material to be used in this research is a case hardening alloy steel called 16MnCr5 manufactured under EN-10084 with DLC hydrogenated coating (a-c: H). Table 1 shows its chemical composition. The cylindrical samples (Ø40 x 15 mm) were thermochemical heat treated [11]. The HV5 hardness measured on the sample surface: average value after carburizing and quenching 805.83 (average deviation 4.303); average value after tempering 732 (average deviation 3.4).

Three group of samples were exposed to a thermal treatment deposition of DLC coating by reactive magnetron sputtering at different temperatures: (i) 180°C (using Ceme-Con C800/9XL deposition chamber), (ii) 200°C and (iii) 250°C (both using Eifeler Vacotec Alpha 400C deposition chamber) [11].

To prepare for the microstructural, electrochemical, and nanoindentation tests, the alloy ingots were divided into three samples (S180, S200, and S250) using a Buehler IsoMet 4000 precision saw (see Fig. 1).

Microstructural analysis, nanoindentation and electrochemical testing, on the embedded samples were performed. The Axio Vert.A1 MAT by ZEISS microscope was utilized for the structural characterization of the samples following the chemical etching process with 3% Nital reagent. The BioLogic Essential SP-150 potentiostat and Sodium chloride solution (10 % NaCl) at 50°C, were utilized for electrochemical experiments employing both continuous and alternate current. This allowed for the determination of the corrosion potential and rate, as well as the performance of electrochemical impedance spectroscopy. The CSM Instruments/Anton Paar NHT2 Durometer is used for nanoindentation testing, with a pressure force range of 0.1 to 500 mN.

Table 1. Composition (in wt%) of the alloys under study according to EN-10084 standard.

C	Cr	Mn	Si	P	S	Fe
0.14 - 0.19	0.8 - 1.1	1 - 1.3	max 0.4	max 0.025	max 0.035	balance

After metallographic examination of the basic material (see Fig. 2), the three samples showed a martensitic structure under both magnifications.

Fig. 3 shows the hardness and modulus of elasticity values with their respective standard deviation (SD) of the three samples studied, where it can be seen that as the heat treatment temperature increases, both hardness and modulus of elasticity tend to decrease. Therefore, specimen S180 has a better wear resistance characteristic compared to the other specimens.

In Fig. 4.a, the corrosion potential (E_{corr}) during the first 5 minutes tends to decrease for samples S180 and S200. However, after one hour of testing, the most stable and positive potential was that of S180. Likewise, the lowest corrosion rate was presented by sample S180, as can be seen in Fig. 4b, since the values of E_{corr} and I_{corr} (corrosion intensity) were lower than those of the other samples.

The equivalent circuit R(QR)(QR), which has two time constants, was used to fit the values obtained by electrochemical impedance spectroscopy (see Fig. 4d). In turn, in the Nyquist (Fig. 4c) and Bode plots (Fig.4e and Fig. 4f) performed at -0.9 V, it

could be observed that the sample showing a more capacitive behavior, in addition to higher impedance and phase angle values, was sample S180.

In this research, the effect of DLC deposition temperature on the microstructure, corrosion resistance in 10% NaCl salt solution at 50°C and mechanical properties of the 16MnCr5 alloy was studied, confirming its martensitic structure for all three samples. In electrochemical and nanoindentation tests, higher corrosion and wear resistance was observed for sample S180, while these parameters tended to decrease at higher DLC deposition temperatures.

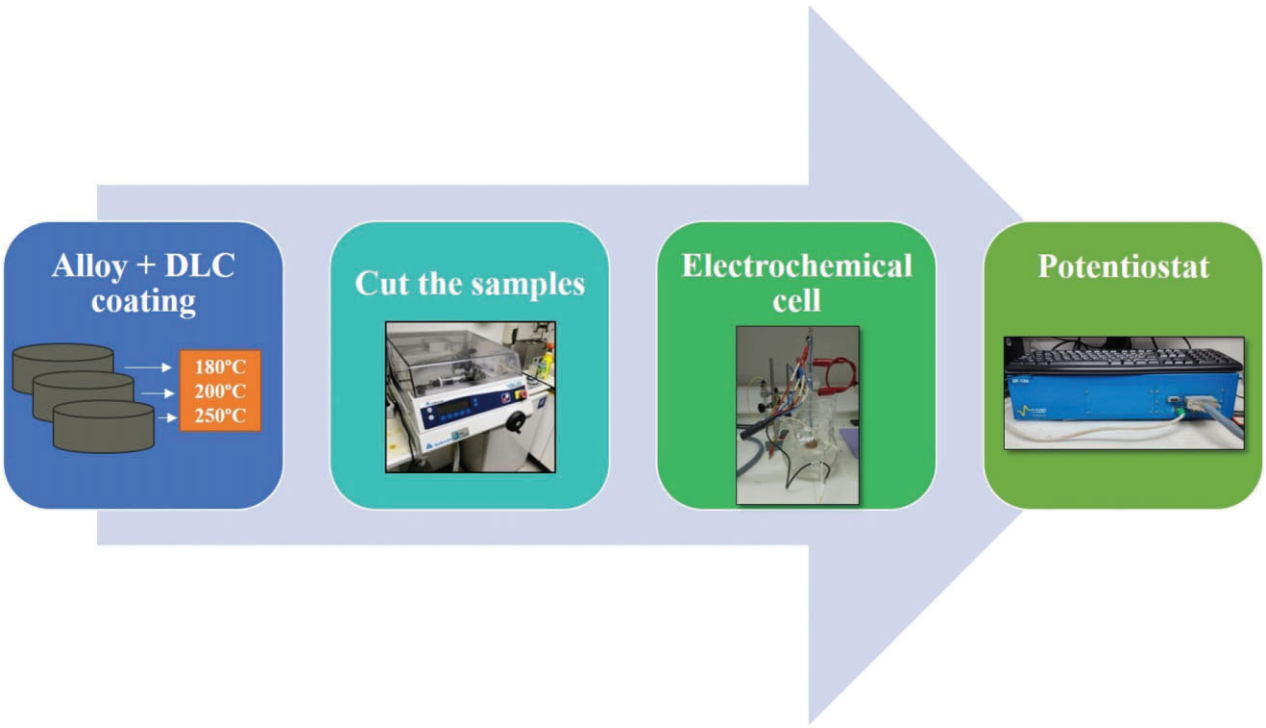

Fig. 1. Preparation of the examined samples.

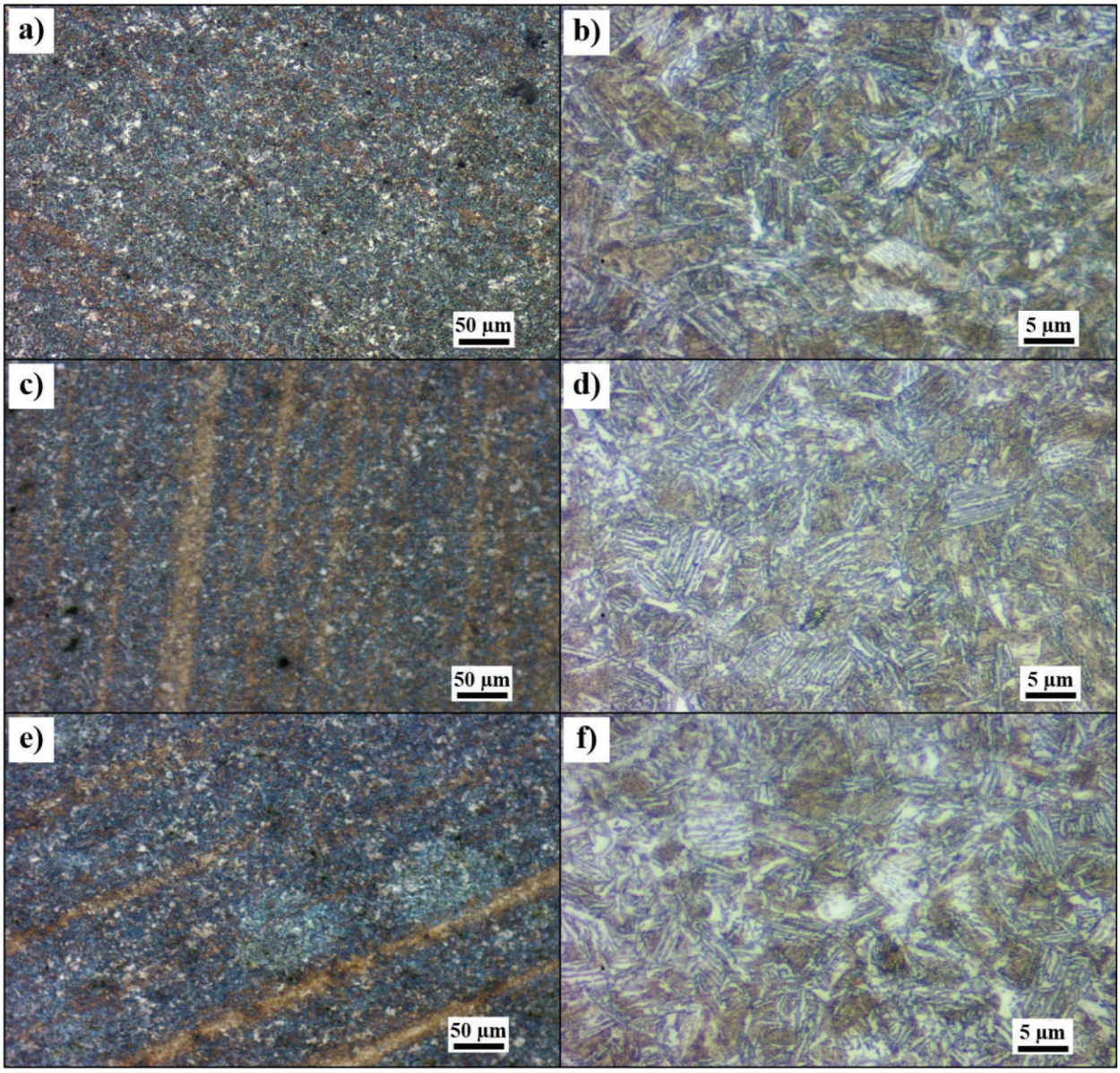

Fig. 2. Microstructure of S180 (a, b), S200 (c, d) and S250 (e, f) samples at x50 and x100 magnifications, respectively.

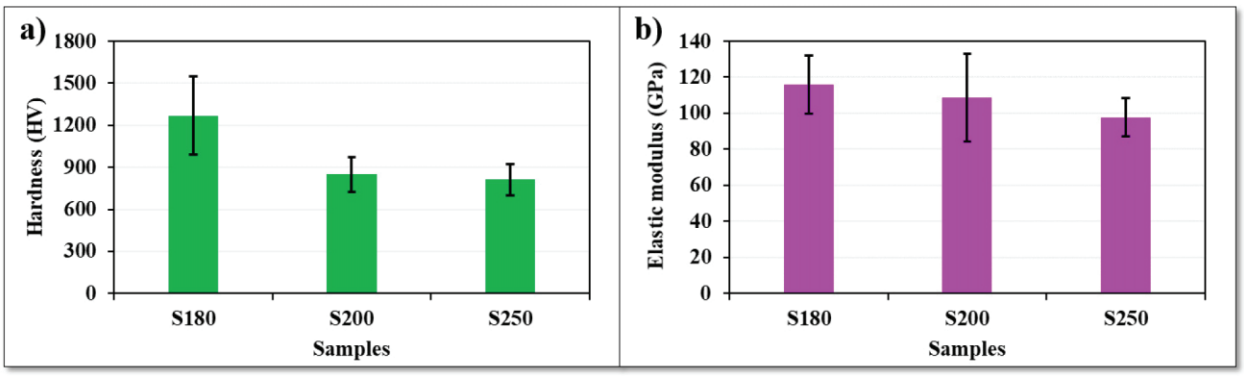

Fig. 3. Hardness and elastic modulus values with SD of the three studied samples.

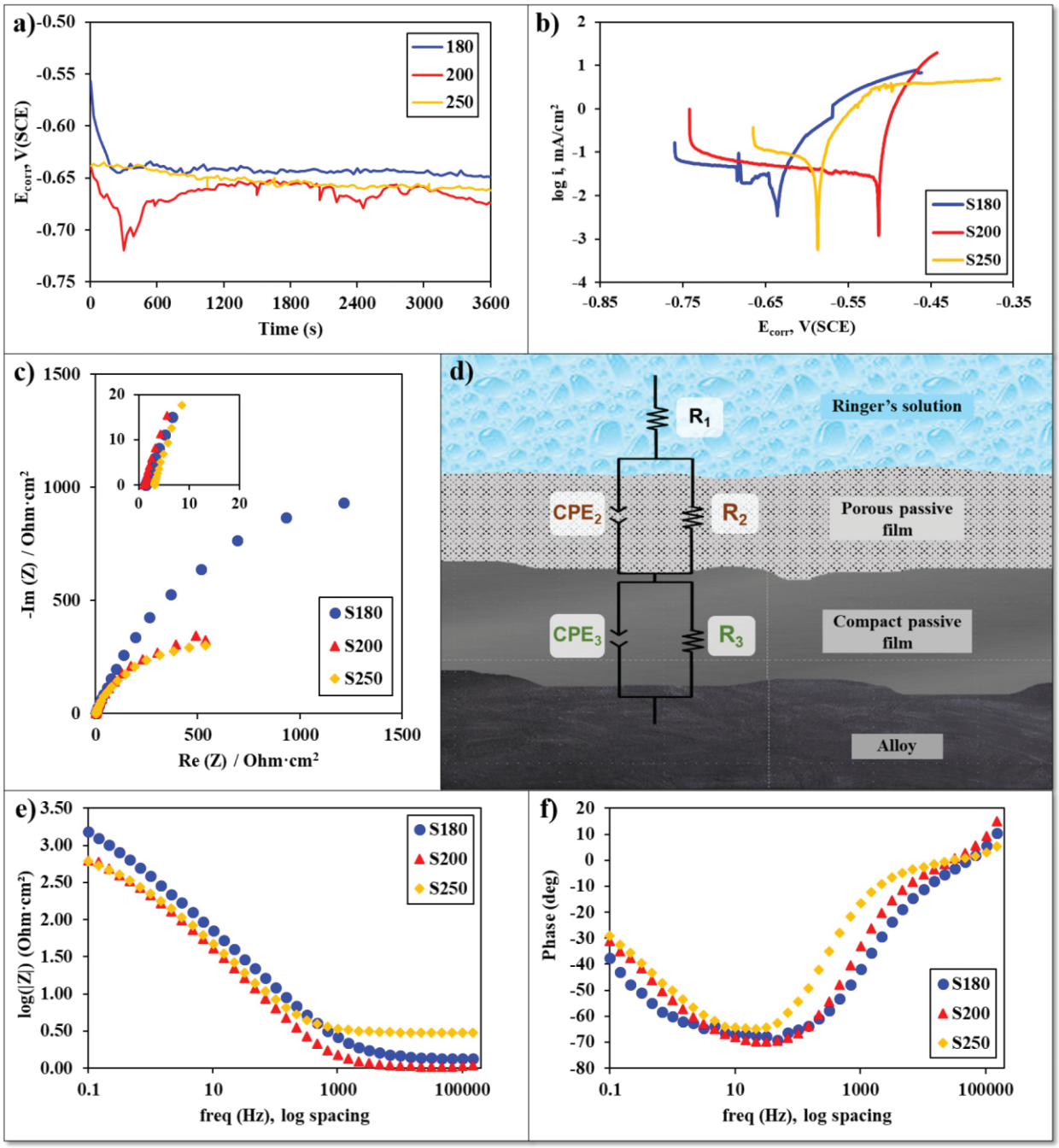

Fig. 4. Corrosion potential (a), corrosion rate (b), Nyquist Diagram (c), equivalent electrical circuit (d), Bode impedance plot (e) and Bode phase plot (f) of the studied samples.

References

1. D. K. Rajak, A. Kumar, A. Behera & P. L. Menezes. *Appl. Sci.* **11**, 4445 (2021) doi:10.3390/app11104445.
2. Q. Zeng & Z. Ning.*Rev. Adv. Mater. Sci.* **60**, 276–292 (2021) doi:10.1515/rams-2021-0028.
3. N. Ohtake *et al. Materials (Basel).* **14**, **315** (2021) doi:10.3390/ma14020315.
4. D. He, S. Zheng, J. Pu, G. Zhang & L. Hu. *Tribol. Int.* **82**, 20–27 (2015) doi:10.1016/j.triboint.2014.09.017.
5. R. Shah *et al. Surf. Coatings Technol.* **487**, **131006** (2024) doi:10.1016/j.surfcoat.2024.131006.
6. W. I. Milne. *Semicond. Sci. Technol.* **18**, S81–S85 (2003) doi:10.1088/0268-1242/18/3/312.
7. M. Zhao *et al. Surf. Coatings Technol.* **484**, **130810** (2024) doi:10.1016/j.surfcoat.2024.130810.
8. T. F. Zhang *et al. Appl. Surf. Sci.* **435**, 963–973 (2018) doi:10.1016/j.apsusc.2017.11.194.
9. S. Viswanathan *et al. J. Mater. Eng. Perform.* **26**, 3633–3647 (2017) doi:10.1007/s11665-017-2783-7.
10. I. Efeoglu, Y. Totik, G. Gulten, B. Yaylali & M. Yesilyurt. *Surf. Coatings Technol.* **495**, **131578** (2025) doi:10.1016/j.surfcoat.2024.131578.
11. D. Feldiorean *et al. Appl. Surf. Sci.* **475**, 762–773 (2019) doi:10.1016/j.apsusc.2019.01.028.